Innovative Polymer Nanocomposite Electrolytes: Nanoscale Manipulation of Ion Channels by Functionalized Graphenes

Bong Gill Choi,[†] Jinkee Hong,[‡] Young Chul Park,[§] Doo Hwan Jung,[§] Won Hi Hong,[†,*] Paula T. Hammond,[‡,*] and HoSeok Park[⊥,*]

[†]Department of Chemical & Biomolecular Engineering (BK21 program), KAIST, Daejeon 305-701, Republic of Korea, [‡]Department of Chemical Engineering, Massachusetts Institute of Technology, Cambridge, Massachusetts 02139, United States, [§]Advanced Fuel Cell Research Center, Korea Institute of Energy Research (KIER) 71-2, Jang-dong, Yusong-gu, Daejeon, Republic of Korea, and [⊥]Department of Chemical Engineering, College of Engineering, Kyung Hee University, 1 Seochon, Giheung-gu, Yongin-si, Gyeonggi-do 446-701, Republic of Korea

ABSTRACT The chemistry and structure of ion channels within the polymer electrolytes are of prime importance for studying the transport properties of electrolytes as well as for developing high-performance electrochemical devices. Despite intensive efforts on the synthesis of polymer electrolytes, few studies have demonstrated enhanced target ion conduction while suppressing unfavorable ion or mass transport because the undesirable transport occurs through an identical pathway. Herein, we report an innovative, chemical strategy for the synthesis of polymer electrolytes whose ion-conducting channels are physically and chemically modulated by the ionic (not electronic) conductive, functionalized graphenes and for a fundamental understanding of ion and mass transport occurring in nanoscale ionic clusters. The functionalized graphenes controlled the state of water by means of nanoscale manipulation of the physical geometry and chemical functionality of ionic channels. Furthermore, the confinement of bound water within the reorganized nanochannels of composite membranes was confirmed by the enhanced proton conductivity at high temperature and the low activation energy for ionic conduction through a Grotthus-type mechanism. The selectively facilitated transport behavior of composite membranes such as high proton conductivity and low methanol crossover was attributed to the confined bound water, resulting in high-performance fuel cells.

KEYWORDS: ion transport · polymer electrolyte · nanocomposite · nanostructure · graphene

At the heart of energy and electrochemical devices, such as fuel cells, solar cells, batteries, supercapacitors, biosensors, and actuators, are polymer electrolytes,[1−5] which conduct ions generated at the electrochemical interfaces *via* either a faradaic or nonfaradaic process.[6,7] Among various polymer electrolytes, Nafion, a perfluoro-sulfonated ionomer, has received significant attention due to its remarkable ionic conductivity and chemical and mechanical stabilities.[1] Accordingly, Nafion, whose structures exhibit a bicontinuous nanostructure composed of a hydrophobic backbone and ionic domains in the hydrated state, has been extensively investigated as a representative polymer electrolyte, along with Nafion composites.[8] In particular, the ions and small molecules within the polymer electrolytes are transported through the interconnected ionic clusters, and as a result, the facilitated transport of target ions is highly desirable for the development of high-performance electrochemical devices.[7,9,10] Therefore, the device and material performances have been shown to be dramatically enhanced by controlling the physical geometry (or size) and chemical functionality (or acidity) of nanoscale ionic clusters in a polymer electrolyte.[11,12]

Recent advances in polymer electrolytes have been directed toward the modification of ionic channels, which is induced by incorporating various nanofillers of functional materials such as metal nanoparticles, inorganic oxides, nanoclay, zeolites, polymers, and carbon nanotubes (CNTs).[13−17] Despite these intensive efforts on the fabrication of polymer nanocomposites, very few studies have demonstrated the enhancement of target ion conduction while suppressing unfavorable ion or mass transport (methanol for direct methanol fuel cells, DMFCs, and gas for proton exchange membrane fuel cells, PEMFCs).[17,18] Indeed, the introduction of ionic moieties of fillers with strong acidic sulfonic groups rather than other functional (hydroxyl, carboxylic, and phosphonic) groups to Nafion can induce higher proton conductivity and thus cause high swelling and methanol crossover through an identical pathway.[8,19] Moreover,

* Address correspondence to whhong@kaist.ac.kr, hammond@mit.edu, phs0727@khu.ac.kr.

Received for review April 9, 2011 and accepted May 2, 2011.

Published online May 02, 2011
10.1021/nn2013113

the permeation of methanol from the anode to the cathode is a critical challenge for the commercialization of DMFCs, as it leads to degraded cell performances *via* a mixed potential as well as the serious fuel loss.[20] Here, we report an innovative strategy for the synthesis of advanced polymer electrolytes whose ion-conducting channels are modulated by functionalized graphenes for facilitated ionic transport.

Recently, graphene oxide (GO), a precursor of reduced graphene oxide (RGO), has been well-known as an excellent amphiphilic soft material due to its oxygen-containing functional groups and chemical tunability of properties.[21−23] The fabrication of polymer and/or inorganic nanocomposites including RGOs and their derivatives is a promising approach for electrical and mechanical applications.[24−28] However, ionic (not electronic) conductive nanocomposites including functionalized graphenes have been unexplored yet. Although there have been a few reports on the fabrication of RGO or GO/Nafion nanocomposites,[27] the ionic transport properties of the resultant materials were not controlled by the introduction of functional groups and practical application into fuel cells has not, to date, been demonstrated.

In this work, sulfonated GOs (SGOs) were incorporated into a Nafion matrix, and the transport properties of the resultant nanocomposites were compared to those of pristine Nafion and GO-incorporated nanocomposites. Importantly, both the desirable size and functionality of ionic clusters through nanoscopic modifications controlled the state of water confined in nanoscale ionic channels. This enabled the unique transport behavior of nanocomposites such as high proton conductivity and low methanol permeability at high temperature and the low activation energy for the proton conduction, resulting in high-performance DMFCs.

RESULTS AND DISCUSSION

Scheme 1 illustrates our strategy for nanoscale physicochemical modification of ionic channels in a Nafion matrix by functionalized graphene. Following previous studies,[29,30] GOs were prepared by the Hummers method. SGOs were obtained from the exfoliated GOs through a microwave-assisted sulfonation method (see Experimental Section). The quality of GOs and SGOs was characterized by transmission electron microscopy (TEM), atomic force microscopy (AFM), X-ray photoelectron spectroscopy (XPS), and FT-IR spectroscopy (see Figures S1−S3 in the Supporting Information). In order to minimize the reduction of size and to maximize the degree of sulfonation through a microwave-assisted functionalization method, we delicately controlled the synthetic parameters such as acid concentration, reaction pressure, and microwave power. The size discrepancy between GOs and SGOs was also minimized by the centrifugal separation, and the transport properties of the composite membranes including microwave-treated GOs were comparable to those of original composite membranes, in the range of ±3% discrepancy (detailed information is provided in Experimental Section). Furthermore, the favorable interactions between the Nafion and SGOs were verified by spectroscopic methods (see Figure S4). The SGO/Nafion (SGON) membranes were obtained from a highly homogeneous solution of Nafion and SGOs in *N*, *N*-dimethylformamide, followed by solution casting. In order to verify the effect of the functionality of ionic channels on the transport properties, GO/Nafion (GON) membranes were prepared as a control sample by the same protocol as employed for the SGON membrane. The proton conductivity and methanol crossover were strongly influenced by the physicochemical properties of the ionic clusters, such as the cluster size and the functional group, as they act as a transport pathway. The physical modification of ionic channels by fillers with two-dimensional nanostructures led to a dramatic decline of unwanted transport such as methanol crossover by means of a barrier and molecular sieve effect;[12] however, the proton conduction may also decrease. Therefore, delicate control of the chemical functionalities of SGOs is expected to be an effective method to enhance the proton transport, while preventing methanol crossover. This is accomplished *via* addition of sulfonic groups for chemical functionality and structural reorganization to reduce cluster size for physical manipulation.

The morphology of the SGON sample was analyzed by TEM and scanning electron microscopy (SEM). Figure 1a presents a TEM image of SGON, which shows a random distribution of SGOs in a Nafion matrix without significant aggregation. This result is consistent with a cross-sectional SEM image of the SGON membrane. After evaporation of the solvents, most of the SGO sheets remained exfoliated and randomly dispersed in the polymer matrix and were tightly held in the Nafion matrix due to the strong interfacial interactions. The mutual interaction between Nafion and SGO and irregular size of fillers made SGO sheets rearrange into the folded state, which results in the smaller size than that of original GO sheets.[31] The as-obtained SGON membranes were macro- and microscopically homogeneous without any cracks (Figure 1b), and enhanced quality of samples arises from the good compatibility between the matrixes and fillers as well as reliable experimental procedures.

An analysis of the microstructure, and its reorganization, of composite membranes was performed by small-angle X-ray scattering (SAXS) and wide-angle X-ray scattering (WAXS) as shown in Figure 1c,d. The hydrated Nafion reveals a clear ionomer peak in SAXS because of the existence of the self-organized ionic cluster networks.[32] Given that the scattering intensity is proportional to the difference in the electron density

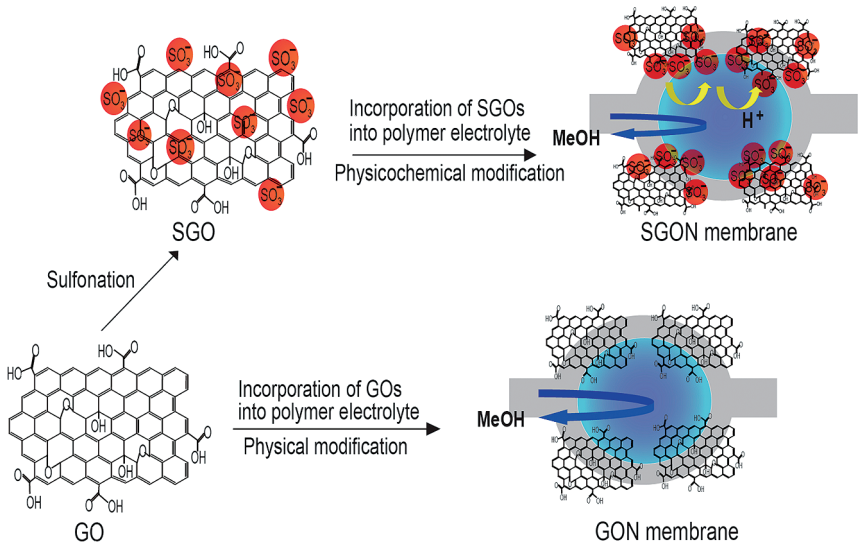

Scheme 1. Physicochemical strategy for realizing tunable transport properties of Nafion membrane using functionalized graphenes.

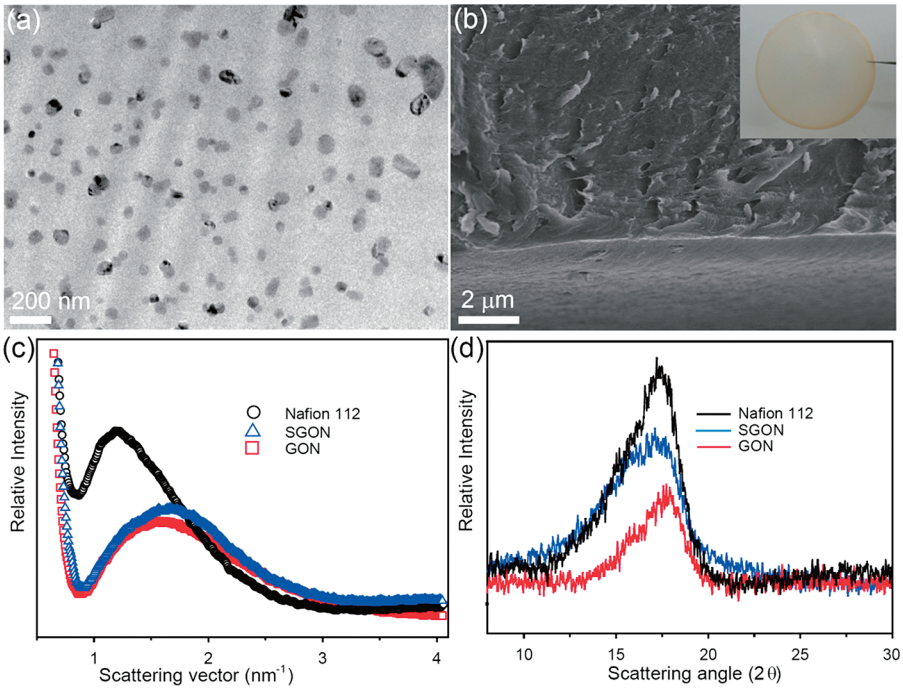

Figure 1. (a) Cross-sectional TEM image of SGON membrane. (b) Cross-sectional SEM and photo (inset) images of SGON membrane and (c) SAXS and (d) WAXD curves of Nafion 112, SGON, and GON membranes.

between backbones and clusters,[33] the intensity reduction of the composite membranes is largely associated with the compatibilizing effect of amphiphilic GO and SGO on the two domains of Nafion by means of the mutual interactions between conjugation and the hydrophobic backbone and between functional groups and hydrophilic clusters. In contrast, the location of the SAXS peak is related to the intercluster distance according to the two-phase model or to the short-range order distance according to the core−shell model.[1] The scattering vector (q) of Nafion was shifted to a larger value compared to that of GON and SGON membranes, respectively. The Bragg spacing (d), which is ascribed to the average dimension of the ionic cluster, was calculated from the following equations:[34] $d = 2\pi/q$ and $q = 4\pi/\lambda \sin\theta$ with a scattering angle 2θ and X-ray wavelength λ. The incorporation of GO and SGO into the Nafion matrix decreased the Bragg spacing from 5.27 to 4.18 and 3.76 nm, respectively, reflecting the shrinkage of ionic clusters through rearrangement of the polymer conformation.[27] Further strong evidence of the structural reorientation was

provided by WAXD, which shows a crystalline reflection of Nafion (indexed as the 100 reflection of the hexagonal structure).[33] The broadening, shift, and intensity decline of the crystalline peak in the composite membranes was attributed to reorganization of the phase-separated structure by means of the incorporation of GO and SGO. It is well-known that the formation of ionic clusters is derived from the counterbalance between the electrostatic energy released by ion–dipole interactions such as $SO_3^- \cdot H^+$ and the elastic free energy attributable to the deformation of backbone chains.[35] In this regard, the changes in the cluster size and the electron density of two domains were triggered by the mutual interactions between the nanofillers and the Nafion matrix, and the different force fields generated distinct optimum cluster size. Therefore, the microstructure of Nafion was rearranged by specific interactions with the functionalized graphene, and as a result, the physical geometry and interaction field of the ionic clusters were controlled by the functional groups of GO or SGO.

A key issue related to variation in the microstructure of ionomers is the transport properties such as proton conductivity and methanol crossover, especially in DMFCs. As shown in Figure 2, the proton conductivity of the SGON membranes is approximately 2-fold higher than that of the Nafion membrane in a temperature range between 298 and 373 K. In comparison to the methanol permeability of the Nafion membrane, that of SGON membranes was significantly reduced by ~35%. The methanol permeability of the GON membranes decreased throughout the measurement range, but their ionic conductivity was similar to that of Nafion membranes. In contrast, SGON membranes showed a unique enhancement of proton conductivity, while decreasing the methanol crossover as a consequence of a reduction of cluster size and/or enhancement of tortuosity in the composite membranes. Considering that appropriate physical and chemical adjustment of the pathway can effectively control ion and mass transport,[1,7,8] these findings indicate the importance of the chemical functionality of nanofillers with respect to the transport properties. Further studies about the influence of other factors such as the density of functional groups and the loading of nanofiller on the transport properties of composite membranes are needed to optimize the DMFC performance.

The exceptional transport behavior by the functionalized graphenes is interpreted here in terms of the state of water confined in nanochannels. The state of water, which is classified into free and bound water, plays a significant role in the transport properties in the membrane.[36,37] The bound water contributes to proton transfer through interaction with sulfonic groups of ionomers, while the free water, which is not bound to the polymer chains, shows behavior similar to that of bulk water.[36] Table 1 displays the state of water in

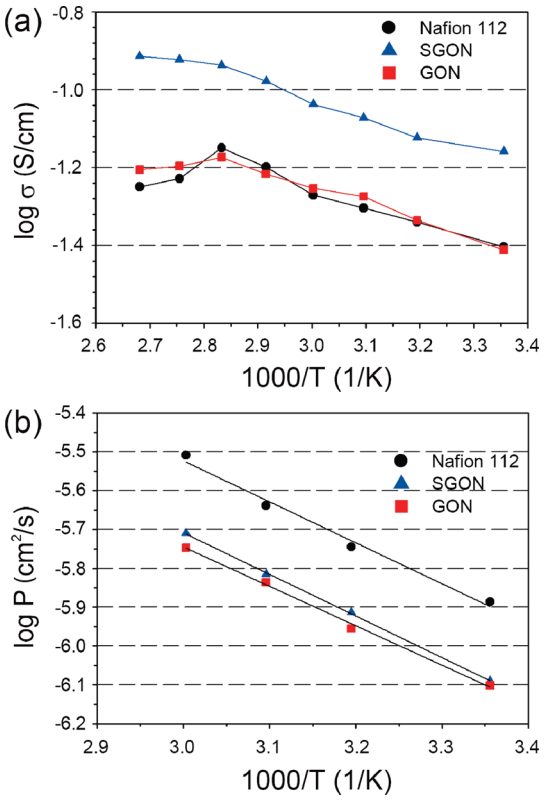

Figure 2. Temperature dependence of (a) proton conductivity and (b) methanol permeability for Nafion 112, SGON, and GON membranes.

Nafion 112, GON, and SGON membranes. The composite membranes exhibited less water uptake than Nafion due to a reduction of free water content, which was attributed to the effective incorporation of SGO into the ionic clusters and the large surface area of SGO because water uptake is strongly influenced by the size of the ionic cluster and the available volume for the occupation of a water molecule.[38] The amount of total, free, and bound water can be expressed as the number of water molecules per sulfonic groups (λ) based on differential scanning calorimeter (DSC) data (see Figure S5 in the Supporting Information)[39,40]

$$\lambda = \frac{n(H_2O)}{n(SO_3^-)} = \frac{WS}{M_w IEC} \quad (1)$$

$$\lambda = \lambda_f + \lambda_b \quad (2)$$

where $n(H_2O)$ is the H_2O mole number, $n(SO_3^-)$ is the SO_3^- group mole number, WS is the weight of water uptake, IEC is the ion exchange capacity, M_w is water's molecular weight, λ is the total hydration number, λ_f is the number of free water molecules per sulfonic groups, and λ_b is the number of bound water molecules per sulfonic groups. Although the size of ionic clusters was reduced, the amount of bound water in the GON membranes was comparable to that of Nafion 112. In particular, the SGON membranes revealed the highest degree of bound water (χ = 95.4%), due to the

TABLE 1. State of Water in Nafion 112, GON, and SGON Membranes

sample	water uptake (wt %)	IEC (equiv/g)	λ (H_2O molecules/SO_3^-)	λ_f (H_2O molecules/SO_3^-)	λ_b (H_2O molecules/SO_3^-)	χ^a (%)
Nafion 112	25.4	0.91	15.5	8.0	7.5	48.4
GON	15.0	0.93	9.0	2.6	6.4	71.1
SGON	18.9	0.97	10.8	0.5	10.3	95.4

[a] $\lambda_b/\lambda \times 100$.

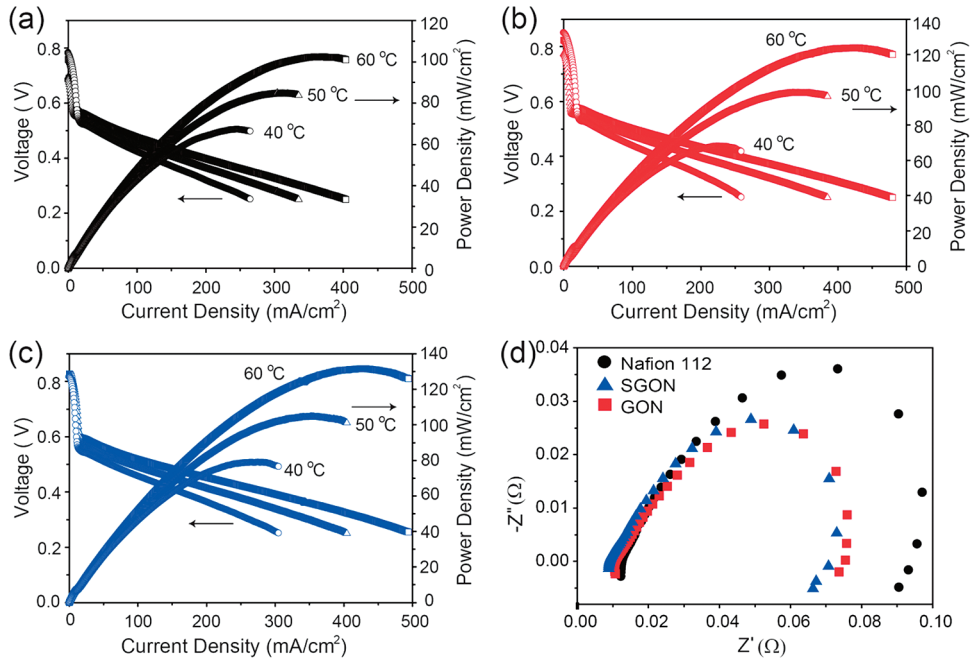

Figure 3. Polarization curves of DMFC single cells obtained from (a) Nafion 112, (b) GO, and (c) SGON membranes under operating temperature of 40, 50, and 60 °C. (d) Nyquist impedance (*Z*) plots for Nafion 112, GO, and SGON membranes.

functionality of sulfonic groups. Remarkably, the ionic conductivity of the SGON membrane increased even above 80 °C, while that of Nafion 112 and GON membranes decreased because of dehydration. The proton conduction of the SGON membranes at high temperature provides clear evidence that the confinement of bound water within the reorganized nanochannels is a consequence of strong interactions between SGO and Nafion. The unique behavior of the SGON membrane by means of bound water confined in nanochannels can be also demonstrated by the temperature dependence of transport properties. The activation energies for transport were calculated from the Arrhenius equation. Despite no significant changes in the activation energies for the methanol permeabilities of the composite membranes, the activation energies for proton conduction were 8.34 kJ/mol for SGON, 8.52 kJ/mol for GON membranes, and 9.18 kJ/mol for Nafion 112. Considering that these values correspond to proton transport through a Grotthus-type mechanism and methanol crossover is strongly influenced by free water,[41] the enhanced proton conductivity and reduced methanol permeability of the SGON membranes are predominantly attributed to the larger portion of bound water than free water.

On the basis of excellent transport properties, the superiority of SGON membranes is demonstrated *via* a single cell test of a DMFC, as shown in Figure 3. The cell performances were evaluated at 40, 50, and 60 °C under fuel cell operating conditions of 1 M methanol at the anode side and for oxygen gas at the cathode side. At the operating temperature, the SGON membranes exhibited better performance than the Nafion 112 and GON membranes. In particular, the maximum power density value of the SGON membrane (132 mW/cm^2) was higher than that of the Nafion 112 (101 mW/cm^2) and GON membranes (120 mW/cm^2) at 60 °C. In order to understand the interfacial behavior of SGON on membrane–electrode assemblies (MEAs), impedance spectroscopy was analyzed. As shown in the Nyquist plot of Nafion 112, GON, and SGON membranes in a frequency range of 10 kHz to 100 mHz, the cell resistance values were 13 mΩ for Nafion, 11 mΩ for GON, and 9 mΩ for SGON membranes. These results indicate that the SGON membranes offered less electrolyte resistance in comparison with those of Nafion 112 and GON membranes, which is in good agreement

with the proton transfer data measured from Figure 2a. In addition, the charge transfer resistance of the SGON membrane, which is proportional to the diameter of a semicircle, was smaller than those of the Nafion 112 and GON membranes. Therefore, the good cell performance of SGON membranes can be attributed to selectively facilitated transport such as high proton conductivity and low methanol crossover.

CONCLUSION

In conclusion, we have demonstrated that the microstructures and physical properties of Nafion can be controlled by the incorporation of functionalized graphenes. In particular, enhanced transport properties and device performances of SGON membranes were achieved by manipulating ionic channels through chemical tuning of the functionality of 2D nanofillers. The chemical strategy delineated herein paves the way to understand the fundamental correlation between the microstructures and transport properties of ionomers as well as to develop the designs of composite and electrolyte membranes with high performance for practical applications.

EXPERIMENTAL SECTION

Chemicals. Graphite powder (<20 μM), hydrazine solution (65 wt % in water), and Nafion (perfluorinated resin solution, 5 wt % in lower aliphatic alcohol and water mixture) were purchased from Aldrich. Sulfuric acid (97%) and nitric acid (70%) aqueous solutions were obtained from Junsei.

Synthesis of Sulfonated Graphene Oxide (SGO). Exfoliated graphene oxide (GO) was prepared by previous report using the modified Hummers method. The preparation of GO sheets was confirmed by TEM and AFM images and XPS and FT-IR spectroscopy results (Figures S1−S3 in the Supporting Information). Considering the irregular size effect of GOs on the performance, GOs were carefully separated by the following procedure. The as-prepared graphite oxide flakes were centrifuged at 4000 rpm for 30 min; the supernatant was recentrifuged at 4000 rpm for 30 min, and these steps were repeated three times for the delicate size selection. Accordingly, we separated solutions into transparent brown upper solution (GO-A) and black sediment (GO-B) according to the size. The GO-A samples were chosen as nanofillers for the fabrication of Nafion-based composite membranes in order to minimize the effect of size on the properties. The synthesis of SGOs was followed by microwave-assisted functionalization method.[42] As-prepared GO-A powder (20 mg) was reacted with a mixture of 10 mL of nitric acid (70%) and 10 mL of sulfuric acid (97%) in the reaction chamber lined with Teflon PFA and controlled with a pressure of 0−200 psi. The GOs functionalized with sulfonic acid groups were obtained after the mixture was then treated with microwave radiation (CEM MDS-2100 microwave digestion system) at 50% of a total of 900 W and 20 psi of pressure for 3 min. The resulting mixture was added with deionized (DI) water (500 mL) carefully (the acid mixture is highly corrosive). The SGO dispersion was purified by dialysis with DI water until the filtrated solution was neutral. Then, the size of SGO was also selected following the identical procedure to GO. The powder of SGO was collected by filtration and dried under vacuum at 60 °C. The preparation of SGOs was performed by TEM, AFM, XPS, and FT-IR (Figures S1−S3 in the Supporting Information). In order to check the size of GOs and SGOs, we calculated the average size of GO and SGO on a basis of 20 batches which includes ~100 samples. The average size of GO-A was 0.272 μm^2, while that of SGO-A was 0.267 μm^2. Although the size of SGO-A after the size selection method was slightly smaller than that of GO-A, the size discrepancy of GO-A and SGO-A (in the range of 2%) was negligible due to the delicate size selection method and the slight damages of GOs during the microwave treatment. Moreover, the minor effect of microwave on the size reduction of GOs was confirmed by checking the changes in the size of GOs, after the same microwave treatment as use in the procedure of SGOs except for the presence of sulfuric and nitric acid. The mean size of microwave-treated GO (MGO-A) flakes was calculated to be 0.269 μm^2 from AFM images. In particular, when the proton conductivity and methanol permeability of GO-A/Nafion (GON-A) and MGO-A/Nafion (MGON-A) membranes were measured, only ±3% discrepancy between the values of the two membranes was observed. These results elucidate that the differences between the transport properties of the isolated GO-A and SGO-A, obtained from the size selection process, were attributed not to the negligible size discrepancy but to the functionality, as confirmed by the very close size of GO-A and SGO-A and the almost same transport properties of GON-A and MGON-A (MGO-A has almost the same size of SGO-A).

SGO Composite Membrane. Nafion solution (perfluorinated resin solution, 5 wt % in lower aliphatic alcohol and water mixture, Aldrich) was dissolved in *N*,*N*-dimethylformamide and added with SGOs (0.5 wt % to Nafion). The mixture was stirred and treated under sonication for 1 h. As-prepared mixture of Nafion and SGOs was slowly poured into a Petri dish in an amount that would give a thickness of *ca.* 50 μm of the formed composite membrane. The filled dish was placed on the leveled plate of a vacuum-dry oven and then was dried by slowly increasing the temperature from 60 to 120 °C for 12 h. The resulting composite membranes were boiled in 30% H_2O_2 for 2 h at 70 °C and then immersed in 1 M H_2SO_4 solution for 1 h. After washing with DI water, the composite membranes were dried at 70 °C under vacuum. GO composite membranes as a control sample were prepared following the same protocols as SGO composite membranes.

Fabrication of Membrane−Electrode Assembly (MEA). The MEA was fabricated using composite membrane, PtRu black (HiSpec 6000TM, Johnson Matthey) for the anode catalyst and Pt black (HiSpec 1000TM, Johnson Matthey) for the cathode catalyst. The catalyst slurry for the electrodes was prepared with the following procedure. In order to prepare the catalyst slurry, the catalyst was mixed with Nafion solution (DuPont, 10 wt %), DI water, isopropyl alcohol, and 1-propanol. The resulting catalyst slurry was painted onto the gas diffusion layers (GDL) by brushing or using a bar-coating method. The GDLs for the anode and the cathode were a carbon paper (TGP-H-060, Toray, Japan) with 5 wt % polytetrafluoroethylene and a carbon sheet (GDL 25BC, SGL Carbon, Germany) with a microporous layer, respectively. The loading of catalysts were 2 mg/cm^2 of PtRu for the anode and 2 mg/cm^2 of Pt for the cathode. The electrode and composite membranes were hot pressed using a Carver Laboratory Press (Model M, USA). The hot pressing of the MEAs was performed at a pressure of less than 50 kg/cm^2 for 60 s at a temperature of 150 °C.

Characterization. TEM images were collected on an EM 912 Ω energy-filtering TEM (EF TEM 120 kV) and a JEM-3010 HR TEM (300 kV) using samples prepared from cross section. In order to observe the dispersion state of SGO sheets in membranes, thin sections (*ca.* 80 nm) were cut by using ULTRACUT UCT ultramicrotome (Leica, Austria), and then the sliced samples were placed on TEM grids. The SAXS experiments were performed at a Rigaku Cu Kα radiation generator. The WAXD data were obtained on a Rigaku D/max IIIC (3 kW) with a θ/θ goniometer equipped with a Cu Kα radiation generator. The diffraction

angle of the diffractograms was in the range of $2\theta = 5-30°$. The proton conductivity of the membranes was measured by ac impedance spectroscopy, based on a Solatron 1255 frequency response analyzer, over a frequency range of 10^{-3} to 10^{6} Hz with 10 mV by a two-point probe method. The conductivity of the sample was obtained from complex impedance analysis. The proton conductivity was calculated by using the equation $\sigma = L/RA$, where σ, L, R, and A are the ionic conductivity, the thickness of the sample, the resistance from the impedance data, and the surface area of the electrode, respectively. The temperature dependence of proton conductivity was carried out by controlling the temperature from 25 to 100 °C. The methanol permeability of membranes was measured by means of the two-compartment diffusion cell under controlled temperature by means of a thermostatic water bath. The concentration of methanol was measured by a refractometer (ATAGO 3T). Measurement of methanol permeability used the two-compartment diffusion cell. One compartment (A) was filled with the mixture of deionized water (50 vol %) and methanol (50 vol %). The other compartment (B) was filled with deionized water. The membrane (area = 4.90 cm^2) was clamped between the two compartments. Concentrations of solutions in the two compartments were controlled constantly using the stirrer in the each cell. As time goes by, the methanol concentration of B cell increases by mass transfer phenomenon attributed to the difference of concentration of methanol. In the constant beginning time, the methanol concentration in compartment A is constant during the experiment, and the rate of mass transfer is kept constantly. Using the above-mentioned assumptions, the concentration of B depending on the function of time was determined according to the following equation:

$$V_B \frac{dC_B}{dt} = A\frac{DK}{L}C_A \quad (3)$$

where C_B and C_A are the concentration of A and B cells; A is the surface area of the membrane; L is the membrane thickness; and D and K are the diffusion coefficient and equilibrium coefficient of methanol, respectively. V is the volume of each cell.

From eq 3 at constant D and K

$$C_B(t) = \frac{AP}{V_B L}C_A(t - t_0) \quad (4)$$

After concentration of B was measured, permeability P, which is the permeability of electrolyte and depends on D and K, was calculated from the slope of the straight line (C_B *versus* time). To analyze the thermal behavior of the Nafion and the composite membranes, differential scanning calorimetry (DSC, DuPont TA 2000) calibrated with indium was used with dried samples. Each sample was first cooled from +25 to −50 °C and then heated at a rate of 5 °C/min to +40 °C. Ion-exchange capacity (IEC) was measured by the classical titration method. The membranes were soaked in 50 mL of 1 M Na_2SO_4 for 24 h. The solutions were then titrated to an end point of pH 7 with 0.01 M NaOH. The IEC of the membranes was calculated by

$$\mathrm{IEC} = \frac{V_A[\mathrm{NaOH}]}{m_{dry} \times 0.001} \quad (5)$$

where V_A is the volume of base required to reach the end point, [NaOH] is the concentration of the base, and m_{dry} is the mass of the dry membrane. All IEC values reported in this work are the average of three titrations. In order to evaluate the performance of the DMFC with composite membranes, the operation conditions were as follows: the anode side of the single cell at the rate of 1.2 cm^3/min for 1 M methanol and the cathode side of the single cell at the rate of 350 cm^3/min for oxygen gas. After 6 days operation upon humidification, all single cell performances were evaluated at 40, 50, and 60 °C. All single cell results were performed three times, and the results presented in this report are the average data.

Acknowledgment. This work was supported by both the National Research Foundation (NRF) funded by the Korean Government (MEST) (20090063004 and NRF-2010-C1AAA001-0029018) and the Technology Innovation Program (10029897, Development of MEA fabrication process using new catalysts and the application technology for direct methanol fuel cell) funded by the Ministry of Knowledge Economy (MKE, Korea).

Supporting Information Available: TEM and AFM images of GO and SGO; XPS and FT-IR spectra of GO and SGO; FT-IR spectra of GON, SGON, and Nafion 112 membranes; DSC heating traces of GON, SGON, and Nafion 112 membranes in order to investigate water state; amount of free and bound water for GON, SGON, and Nafion 112 membranes calculated from DSC curves. This material is available free of charge *via* the Internet at http://pubs.acs.org.

REFERENCES AND NOTES

1. Mauritz, K. A.; Moore, R. B. State of Understanding of Nafion. *Chem. Rev.* **2004**, *104*, 4535–4585.
2. Wong, W.-Y.; Wang, X.-Z.; He, Z.; Djurišić, A. B.; Yip, C.-T.; Cheung, K.-Y.; Wang, H.; Mak, C. S. K.; Chan, W.-K. Metallated Conjugated Polymers as a New Avenue towards High-Efficiency Polymer Solar Cells. *Nat. Mater.* **2007**, *6*, 521–527.
3. Tarascon, J.-M.; Armand, M. Issues and Challenges Facing Rechargeable Lithium Batteries. *Nature* **2001**, *414*, 359–367.
4. Armand, M.; Endres, F.; MacFarlane, D. R.; Ohno, H.; Scrosati, B. Ionic-Liquid Materials for the Electrochemical Challenges of the Future. *Nat. Mater.* **2009**, *8*, 621–629.
5. Ding, J.; Qing, W. Current-Driven Ion Fluxes of Polymeric Membrane Ion-Selective Electrode for Potentiometric Biosensing. *J. Am. Chem. Soc.* **2009**, *131*, 14640–14641.
6. Simon, P.; Gogotsi, Y. Materials for Electrochemical Capacitors. *Nat. Mater.* **2008**, *7*, 845–854.
7. Maier, J. Nanoionics: Ion Transport and Electrochemical Storage in Confined Systems. *Nat. Mater.* **2005**, *4*, 805–815.
8. Devanathan, R. Recent Developments in Proton Exchange Membranes for Fuel Cells. *Energy Environ. Sci.* **2008**, *1*, 101–119.
9. Bussian, D. A.; O'Dea, J. R.; Metiu, H.; Buratto, S. K. Nanoscale Current Imaging of the Conducting Channels in Proton Exchange Membrane Fuel Cells. *Nano Lett.* **2007**, *7*, 227–232.
10. Park, M. J.; Downing, K. H.; Jackson, A.; Gomez, E. D.; Minor, A. M.; Cookson, D.; Weber, A. Z.; Balsara, N. P. Increased Water Retention in Polymer Electrolyte Membranes at Elevated Temperatures Assisted by Capillary Condensation. *Nano Lett.* **2007**, *7*, 3547–3552.
11. Miyatake, K.; Tombe, T.; Chikashige, Y.; Uchida, H.; Watanabe, M. Enhanced Proton Conduction in Polymer Electrolyte Membranes with Acid-Functionalized Polysilsesquioxane. *Angew. Chem., Int. Ed.* **2007**, *46*, 6646–6649.
12. Choi, Y. S.; Kim, T. K.; Kim, E. A.; Joo, S. H.; Pak, C.; Lee, Y. H.; Chang, H.; Seung, D. Exfoliated Sulfonated Poly(arylene ether sulfone)−Clay Nanocomposites. *Adv. Mater.* **2008**, *20*, 2341–2344.
13. Shao, Z.-G.; Joghee, P.; Hsing, I. Preparation and Characterization of Hybrid Nafion−Silica Membrane Doped with Phosphotungstic Acid for High Temperature Operation of Proton Exchange Membrane Fuel Cells. *J. Membr. Sci.* **2004**, *229*, 43–51.
14. Joo, S. H.; Park, C.; Kim, E. A.; Lee, Y. H.; Chang, H.; Seung, D.; Choi, Y. S.; Park, J.-B.; Kim, T. K. Functionalized Carbon Nanotube−Poly(arylene sulfone) Composite Membranes for Direct Methanol Fuel Cells with Enhanced Performance. *J. Power Sources* **2008**, *180*, 63–70.
15. Chen, Z.; Holmberg, B.; Li, W.; Wang, X.; Deng, W.; Munoz, R.; Yan, Y. Nafion/Zeolite Nanocomposite Membrane by *In Situ* Crystallization for a Direct Methanol Fuel Cell. *Chem. Mater.* **2006**, *18*, 5669–5675.
16. Choi, B. G.; Park, H.; Im, H. S.; Kim, Y. J.; Hong, W. H. Influence of Oxidation State of Polyaniline on Physicochemical and Transport Properties of Nafion/Polyaniline Composite Membrane for DMFC. *J. Membr. Sci.* **2008**, *324*, 102–110.

17. Kannan, R.; Kakade, B. A.; Pillai, V. K. Polymer Electrolyte Fuel Cells Using Nafion-Based Composite Membranes with Functionalized Carbon Nanotubes. *Angew. Chem., Int. Ed.* **2008**, *47*, 2653–2656.
18. Chai, Z.; Wang, C.; Zhang, H.; Doherty, C. M.; Ladewig, B. P.; Hill, A. J.; Wang, H. Nafion–Carbon Nanocomposite Membranes Prepared Using Hydrothermal Carbonization for Proton-Exchange Membrane Fuel Cells. *Adv. Funct. Mater.* **2010**, *20*, 4394–4399.
19. Wang, H.; Holmberg, B. A.; Huang, L.; Wang, Z.; Mitra, A.; Norbeck, J. M.; Yan, Y. Nafion–Bifunctional Silica Composite Proton Conductive Membranes. *J. Mater. Chem.* **2002**, *12*, 834–837.
20. Paik, Y.; Kim, S.-S.; Han, O. H. Methanol Behavior in Direct Methanol Fuel Cells. *Angew. Chem., Int. Ed.* **2007**, *47*, 94–96.
21. Dreyer, D. R.; Park, S.; Bielawski, C. W.; Ruoff, R. S. The Chemistry of Graphene Oxide. *Chem. Soc. Rev.* **2010**, *39*, 228–240.
22. Cote, L. J.; Kim, F.; Huang, J. Langmuir–Blodgett Assembly of Graphite Oxide Single Layers. *J. Am. Chem. Soc.* **2009**, *131*, 1043–1049.
23. Kim, J.; Cote, L. J.; Kim, F.; Yuan, W.; Shull, K. R.; Huang, J. Graphene Oxide Sheets at Interfaces. *J. Am. Chem. Soc.* **2010**, *132*, 8180–8186.
24. Liang, J.; Huang, Y.; Zhang, L.; Wang, Y.; Ma, Y.; Guo, T.; Chen, Y. Molecular-Level Dispersion of Graphene into Poly(vinyl alcohol) and Effective Reinforcement of Their Nanocomposites. *Adv. Funct. Mater.* **2009**, *19*, 2297–2302.
25. Xu, Y.; Hong, W.; Bai, H.; Li, C.; Shi, G. Strong and Ductile Poly(vinyl alcohol)/Graphene Oxide Composite Films with a Layered Structure. *Carbon* **2009**, *47*, 3538–3543.
26. Kim, H.; Miura, Y.; Macosko, C. W. Graphene/Polyurethane Nanocomposites for Improved Gas Barrier and Electrical Conductivity. *Chem. Mater.* **2010**, *22*, 3441–3450.
27. Ansari, S.; Kelarakis, A.; Estevez, L.; Giannelis, E. P. Oriented Arrays of Graphene in a Polymer Matrix by *In Situ* Reduction of Graphite Oxide Nanosheets. *Small* **2010**, *6*, 205–209.
28. Bao, Q.; Zhang, H.; Yang, J.; Wang, S.; Tang, D. Y.; Jose, R.; Ramakrishna, S.; Lim, C. T.; Loh, K. P. Graphene–Polymer Nanofiber Membrane for Ultrafast Photonics. *Adv. Funct. Mater.* **2010**, *20*, 782–791.
29. Hummers, W. S.; Offeman, R. E. Preparation of Graphite Oxide. *J. Am. Chem. Soc.* **1958**, *80*, 1339.
30. Choi, B. G.; Park, H.; Park, T. J.; Yang, M. H.; Kim, J. S.; Jang, S.-Y.; Heo, N. S.; Lee, S. Y.; Kong, J.; Hong, W. H. Solution Chemistry of Self-Assembled Graphene Nanohybrids for High Performance Flexible Biosnesors. *ACS Nano* **2010**, *4*, 2910–2918.
31. Ramanathan, T.; Abdala, A. A.; Stankovich, S.; Dikin, D. A.; Herrera-Alonso, M.; Piner, R. D.; Adamson, D. H.; Schniepp, H. C.; Chen, X.; Ruoff, R. S.; *et al.* Functionalized Graphene Sheets for Polymer Nanocomposites. *Nat. Nanotechnol.* **2008**, *3*, 327–331.
32. Schmidt-Rohr, K.; Chen, Q. Parallel Cylindrical Water Nanochannels in Nafion Fuel-Cell Membranes. *Nat. Mater.* **2008**, *7*, 75–83.
33. Fujimura, M.; Hashimoto, T.; Kawai, H. Small-Angle X-ray Scattering Study of Perfluorinated Ionomer Membranes. 1. Origin of Two Scattering Maxima. *Macromolecules* **1981**, *14*, 1309–1315.
34. Gierke, T. D.; Munn, G. E.; Wilson, F. C. The Morphology in Nafion Perfluorinated Membrane Products, As Determined by Wide- and Small-Angle X-ray Studies. *J. Polym. Sci., Polym. Phys. Ed.* **1981**, *19*, 1687–1704.
35. Eisenberg, A. Clustering of Ions in Organic Polymers. A Theoretical Approach. *Macromolecules* **1970**, *3*, 147–154.
36. Kim, Y. S.; Dong, L.; Hickner, M. A.; Glass, T. E.; Webb, V.; McGrath, J. E. State of Water in Disulfonated Poly(arylene ether sulfone) Copolymers and a Perfluorosulfonic Acid Copolymer (Nafion) and Its Effect on Physical and Electrochemical Properties. *Macromolecules* **2003**, *36*, 6281–6285.
37. Siu, A.; Schmeisser, J.; Holdcroft, S. Effect of Water on the Low Temperature Conductivity of Polymer Electrolytes. *J. Phys. Chem. B* **2006**, *110*, 6072–6080.
38. Asaka, K.; Fujiwara, N.; Oguro, K.; Onishi, K.; Sewa, S. State of Water and Ionic Conductivity of Solid Polymer Electrolyte Membranes in Relation to Polymer Actuators. *J. Electroanal. Chem.* **2001**, *505*, 24–32.
39. Tamura, T.; Kawakami, H. Aligned Electrospun Nanofiber Composite Membranes for Fuel Cell Electrolytes. *Nano Lett.* **2010**, *10*, 1324–1328.
40. Wu, H.-L.; Ma, C.-C.; Li, C.-H.; Lee, T.-M.; Chen, C.-Y.; Chiang, C.-L.; Wu, C. Sulfonated Poly(ether ether ketone)/Poly(amide imide) Polymer Blends for Proton Conducting Membrane. *J. Membr. Sci.* **2006**, *280*, 501–508.
41. Kreuer, K.-D. Proton Conductivity: Materials and Applications. *Chem. Mater.* **1996**, *8*, 610–641.
42. Choi, B. G.; Park, H.; Yang, M. H.; Jung, Y. M.; Lee, S. Y.; Hong, W. H.; Park, T. J. Microwave-Assisted Synthesis of Highly Water-Soluble Graphene towards Electrical DNA Sensor. *Nanoscale* **2010**, *2*, 2692–2697.